RESULTS AND USE OF NON-LINEAR BEHAVIOR BETWEEN LENGTH AND BOND FRICTION OF FULLY GROUTED ROCK BOLTS IN SELECTED JOINTED ROCK MASSES

Ondřej HOLÝ
Institute of Geotechnics, Faculty of Civil Engineering, Brno University of Technology,
Veveří 331/95 602 00, Brno
Tel.: +420724562173, E-mail: holy@geotechnikaholy.cz

ABSTRACT

The anchor length d_b of rock bolts is often determined empirically by the insertion of the bond friction constant τ_b at the grout-rock interface. The relationship between force F_b by limit bond stress and bond length (or bond area) is their ratio. Within the same location, the anchor length can be overestimated or underestimated by usage τ_b = constant. In this paper, the results of load tests of passive rock bolts were analyzed across the many rocks of the Bohemian Massif using selected parameters (*RQD* index, *GSI* values, bulk density ρ_v, uniaxial compressive strength *UCS*) and their correlation. It was found that the relationship between the anchor length and the limit bound friction is non-linear and is influenced by selected parameters and the type of anchor grouting material (cement and resin). It was considered a state where $\tau_b = \boldsymbol{f}$ (d_b, F_b, ρ_v, *UCS*, *RQD*, *GSI*) for 3 types of bonding (1-cement sealing, 2-cement grouting, 3-mixing of resin cartridge). The achieved and measured bond friction was verified by solving the polynomial roots using the CG (conjugate gradient) method. The accuracy of the results reached the maximum mean difference value abs$\Delta\tau_b$ = 0.02 MPa and the standard deviation SD = 0.058. With this verified model, a simulation of random variables was performed by the Monte Carlo method for F_b = const. with the uniform and normal distribution with n = 1500 samples. The results were converted to diagrams represented by the mean value of the uniform distribution (best fit curves) and the normal distribution envelope curves (for 3σ).

Keywords: bond stress; geological strength index; rock bolts; resin; anchor length

1 INTRODUCTION

Within the research project, an extensive phase of field load tests of rock bolts was carried out. The tests were conducted at 12 locations with varied joint rock masses of the Bohemian Massif. Before the initial tests, a loading stand was designed and constructed. A total of 201 pieces of tensile tests of bolts having bond lengths from 0.5 up to 2.5 m, a diameter of 22-32 mm, were performed. These were steel fully threaded rods (C), steel self-drilling rods (I), and fiberglass rods (R). The bolts were bonded into the cement (E) grout and resin (L, equiv. G). The loading tests were always performed until the material failure of bolts or shear stress failure at the interface of cement-rock. At each location, basic geotechnical survey was carried out in the form of drill core diameter of 50 mm in a length of 3.0 meters with the assessment of the rock mass properties in situ, and laboratory testing of rock mechanics. Upon the completion of the testing protocols, the rock mass properties analysis was performed focusing on the evaluation of the bond friction (bond stress equivalent) τ_b [MPa] at the grouting-rock interface. The detailed scope and description of the loading tests was published by Holý [1].

Of all performed loading tests, 87 pieces were used for further evaluation, i.e. about 43%. The interpretation of the results was not focused on the deformation parameters, but the evaluation of the progressive load vs. displacement. From the course of the tests, the limit of the full mobilization of the shear friction was assessed before the yield strength (in case of C and I rods) or the strength of the composite thread (in case of R).

Since the end of the project in 2016 and the publishing of the results by Holý [1], a critical review of the data and the search for wider relations has been performed, mainly towards the character of rock discontinuities of all 12 localities (Fig. 1). In addition, another 6 localities (rock mass properties only) were added, where the author carried out a similar geotechnical survey in the framework of work orders (Tab. 1).

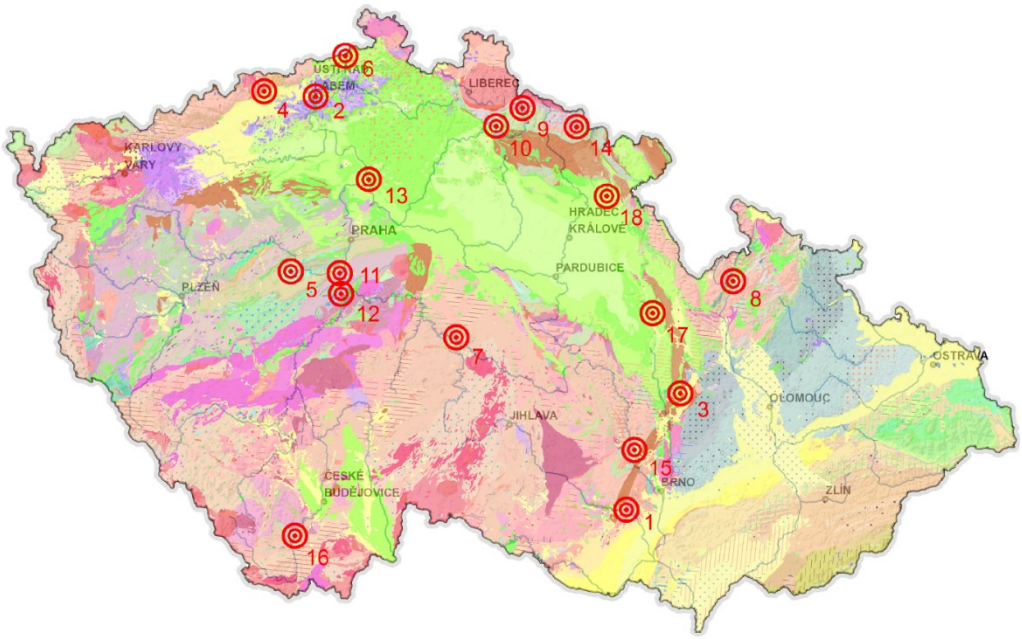

Fig. 1 Situation of the tested (no.1-12) and complementary (no.13-18) localities in the map of the regional-geological division of the Czech Republic 1:500 000 [www.geology.cz].

The interpretation of loading curves (Fig. 2) is based on the observation of bolt behaviour in two phases A and B. In the phase A, the linear elastic deformation of the free end of the bolt is observed, which extends into the phase B by decreasing the tensile force (and stiffness) and softening.

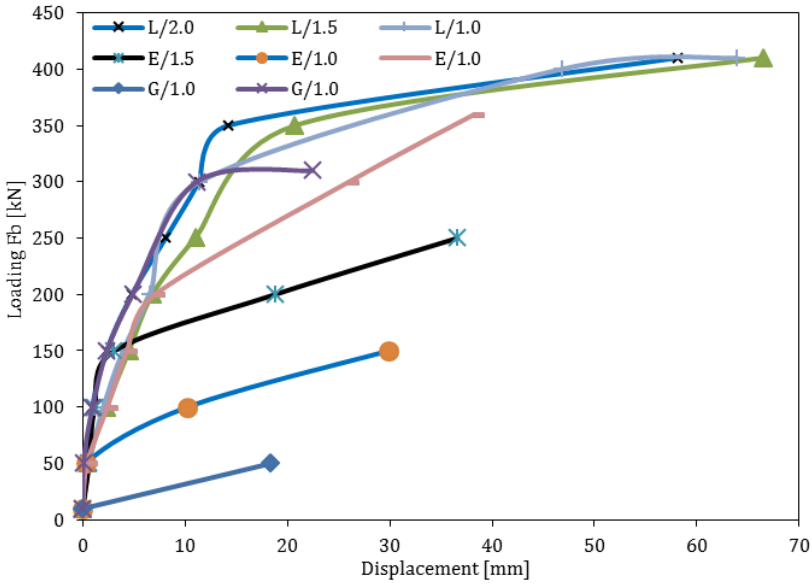

Fig. 2 Example of loading curves of fully threaded rods in bond type E and L eq. G (value behind a stroke indicates bond length), background picture shows pulling out of cement grout in radial jointed slate.

If a deviation from the linear portion of the curve to the yield strength of the bolt or the strength of the thread occurred, the shear friction was mobilized at the given point by breaking the cohesion at the boundary of the grout/bolt or grout/wall of the borehole. This phenomenon was visually validated after each test (see Fig. 2). It is advisable to state that in many cases the yield strength and the ultimate limit strength of the rods exceeded the manufacturer's data. These results as well as the tests with failure at the bolt/grout interface have not been further evaluated. The selected load curves were fitted by a high order polynomial, and using tangent (derivation) on the linear portion of the curve whose failure point was found. It was often possible to use a bilinear fit with a point of intersection at the point where the force drop was found.

Table 1. Summary of locations and their basic characteristics

N. of location	Location	Petrographic rock type	*UCSmean* [MPa]	*ρvmean* [kg.m^{-3}]	*Correlated UTS##* [MPa]	*RQDmean* [%]	*GSI* [-]	*Qrate* [m^2.s^{-2}]
1	Dolní Kounice	Granodiort, type Tetčice	74	2618	7.2	41	52	35.4
2	Ústí n. Labem – Mariánská rock	Trachyte	65	2423	6.5	51***	65.9	37.3
3	Velké Opatovice	Sandy marlite	55	2152	1.4	76	56	39.1
4	Hrob	Two-mica paragneiss	29*	2519*	1.7*	13***	32.8	86.7
5	Big open pit mine Čertovy Schody	Micrite limestone	51	2669	1.3	68	64	52.3
6	Dolní Žleb	Quartzy sandstone	31	2016	0.9	73	59.9	65
7	Quarry Vlastějovice	Orthogneiss, scarn	66	2579	6.1	24	41.1	39.1
8	Hanušovice	Amphibolite	62	2869	5.6	39	48.6	46.3
9	Vilémov	Phyllite to quarzite	50	2628	3.9	52	57.5	52.6
10	Železný Brod	Two-mica phyllite	29**	2535**	0.1**	21***	28	87.4
11	Vrané nad Vltavou	Tuffite	86	2627	2	83	70.6	30.5
12	Štěchovice	Slate	29	2690	0.9	68	67	92.8
13#	Mělník – Na Polabí	Calciferous marlite	20	2288	0.7	57	39	114.4
14#	Pomezní Boudy	Gneiss	77	2642	7.8	71	-	34.3
15#	Tišnov - Trmačov	Arcose	53	2641	1.4	58	-	49.8
16#	Český Krumlov J1	Crystalline limestone	46	2838	3.4	100	-	61.7
17#	Český Krumlov J2	Crystalline limestone	106	2822	13.1	65	-	26.6
18#	Český Krumlov J3	Crystalline limestone	103	2841	12.5	100	-	27.6
19#	Český Krumlov J4	Crystalline limestone	86	2851	9.3	53	-	33.2
20#	Český Krumlov J5	Crystalline limestone	102	2851	12.3	80	-	28
21#	Dlouhá Třebová V1	Calciferous marlite	66	2531	1.6	50	-	38.3
22#	Dlouhá Třebová V2	Calciferous marlite	101	2427	2.2	54	-	24
23#	Česká Skalice 1	Calciferous marlite	100	2569	2.2	76	-	25.7
24#	Česká Skalice 2	Calciferous marlite	74	2495	1.7	50	-	33.7

Note: *) 2 samples, **) 1 sample by Schmidt hammer, ***) by Palmström [2], #) supplementary localities (author´s well file), ##) by Kim and Lade [3], *Qrate:* ratio of *ρvmean* and *UCSmean; RQDmean* by Deer [4]

2 BASIC AND HEURISTIC MODEL OF BOND FRICTION

A shear stress τ [Pa] is generally the component of stress coplanar with a material area A' [m.m] and arises from the force vector F [N] component parallel to this cross section. The basic bond friction model of a rock bolt is given by $\tau_b = F_b/A'$ [MPa] where F_b [kN] represents the limit failure force with fully mobilized τ_b and $A' = 0.002\pi r_b d_b$ [m^2] represents the area of bonding material in the borehole with a diameter of r_b [mm] with the given bond length d_b [m]. The value of the bond stress can be obtained, in addition to load tests, by estimation according to Littlejohn and Bruce [5] as $\tau_b = UCS/30$ or by using the table data, see Tab. 2

Table 2. Allowable rock–grout bond stresses in cement grout anchorages

Rock description	*UCS range [MPa]*	*Allowable bond stress [MPa]*
Strong rock	> 100	1.05-1.40
Medium rock	50-100	0.7-1.05
Weak rock	20-50	0.35-0.7
Rock type		
Granite, basalt		0.55-1.0
Dolomitic limestone		0.45-0.70
Soft limestone		0.35-0.50
Slates, strong shales		0.30-0.45
Weak shales		0.05-0.30
Sandstone		0.30-0.60
Concrete		0.45-0.90

Note: modified by Wyllie [6]

It is worth noting that the average bond friction is considered in the following text, although its highly non-uniform distribution along the bond length was derived by Li and Stillborg [7].

The chosen heuristic model here was a search for such approximate solution where $\tau_b = \boldsymbol{f}(d_b, F_b, \rho_v, UCS, RQD, GSI)$ for 3 types of bonding material (technology). The influence of three genetic types of rocks (magmatic, sedimentary and metamorphic) was suppressed and, on the contrary, the parameters of its own jointed rock mass were taken into account. The verification of the model should achieve the accuracy ideally $\pm(\tau_{approx} - \tau_{experim}) \rightarrow 0$. In the first step the calculation of certain massiveness of rock masses was carried out (see Tab. 1) by factor

$$Q_{rate} = \rho_{vmean}/UCS_{mean} \tag{1}$$

and its graphical comparison with RQD_{mean} and GSI is shown in Fig. 3a,b.

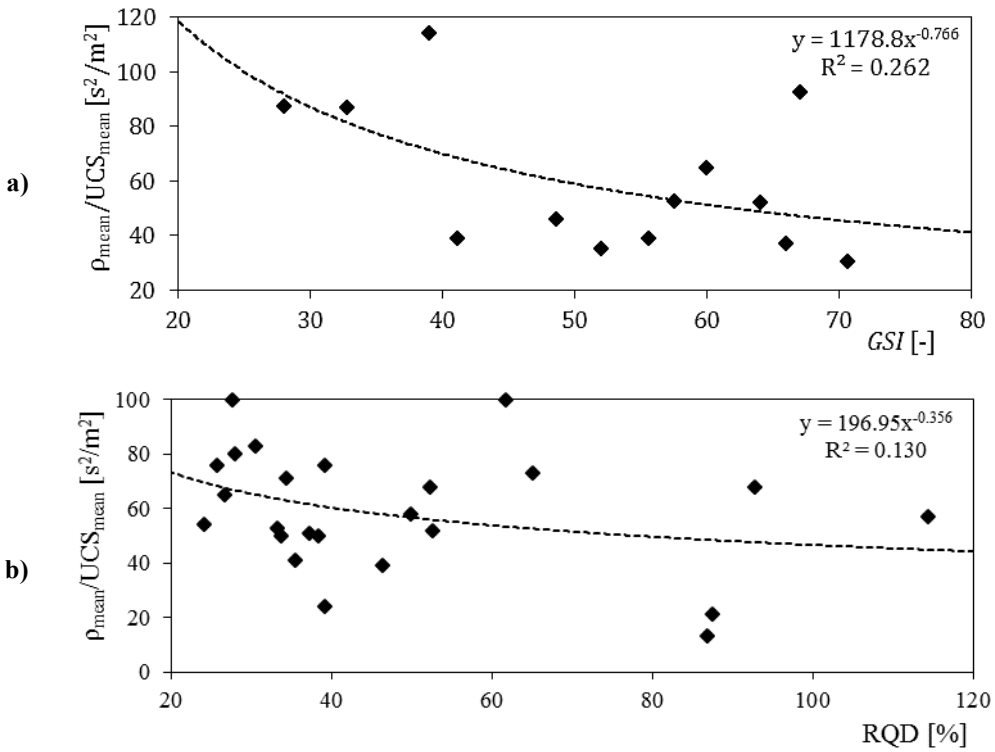

Fig. 3 Dependence between Q_{rate} ratio and GSI (a) and RQD_{mean} (b)

Although the obtained approximation is not too strong, it was used as a sufficient for the next process. We will make a substitution in accordance with Fig. 3a,b, as:

$$Q_{rate} = 196.95\ RQD_{mean}{}^{-0.356} \xrightarrow{subst.} q = f(RQD_{mean}) \tag{2}$$

and

$$Q_{rate} = 1178.79\ GSI^{-0.766} \xrightarrow{subst.} q' = f(GSI) \tag{3}$$

where q and q' represent correlation functions. In the second step, a separate data analysis was performed for each load test (Tab. 3). The RQD_w index was newly defined as the weighted value according to the bond length and each drill core meter.

The value of GSI is given in relationship $GSI = 1.5\ J_{Cond89} + 0.5\ RQD_w$, adopted by Hoek et al. [8] where $J_{Cond89} = 35\ J_r/J_a/(1+J_r/J_a)$ is Joint Condition rating after Bieniawski in Hoek et al. [8]. Substitution of this relationship into first equation yields:

$$GSI = \frac{52 J_r/Ja}{(1+J_r/J_a)} + RQD_w/2 \tag{4}$$

where (J_r/J_a) quotient represents the roughness and frictional characteristics of the joint walls.

Table 3. Data base of model's input parameters

Loading diagram code	$2r_b$ [mm]	db [m]	Rod type	Bond type	rr [mm]	$RQDw$ [%]	τb [MPa]	Fb [kN]	ε [%]	Jr [-]	Ja [-]	$JCond89$ [-]	GSI [-]	Functions q	p	q'	p'
L10-S10	36	1	C	E	22	44	0.50	56	0.02	2	4	11.7	39.5	51.20	56.01	70.54	0.007
L10-S11	36	0.8	C	E	22	33	0.44	37	0.01	2	4	11.7	34.0	56.72	49.34	79.13	0.006
L4-S13	36	2	C	E	22	9	0.34	76	0.02	2	2	17.5	30.8	90.08	38.00	85.46	0.004
L4-S17	51	1	C	E	22	11	0.36	57	0.02	2	2	17.5	31.8	83.87	57.00	83.39	0.004
L7-S5	36	1.5	C	E	22	32	0.32	54	0.02	2.5	2	19.4	45.2	57.35	36.01	63.66	0.005
L8-S16	36	1	C	E	22	36	0.92	104	0.03	2.5	2	19.4	47.2	54.99	104.02	61.58	0.015
L9-S9	36	0.5	C	E	22	38	1.10	62	0.02	3	3	17.5	45.3	53.95	124.02	63.57	0.017
L10-S13	51	1	I	E	32	44	0.92	148	0.02	2	4	11.7	39.5	51.20	148.02	70.54	0.013
L10-S14	51	0.8	I	E	32	33	0.54	65	0.01	2	4	11.7	34.0	56.72	86.68	79.13	0.007
L10-S15	51	0.5	I	E	32	22	0.95	76	0.01	2	4	11.7	28.5	65.53	152.01	90.58	0.010
L8-S19	51	1.5	I	E	32	43	0.50	119	0.02	2.5	2	19.4	50.7	51.62	79.34	58.29	0.008
L8-S20	51	1	I	E	32	36	0.34	54	0.01	2.5	2	19.4	47.2	54.99	54.01	61.58	0.005
L10-S4	36	1	R	E	25	44	0.67	76	0.08	2	4	11.7	39.5	51.20	76.01	70.54	0.010
L4-S7	36	1.5	R	E	25	9	0.36	61	0.06	2	2	17.5	30.8	90.08	40.67	85.46	0.004
L4-S9	36	1	R	E	25	11	1.09	123	0.13	2	2	17.5	31.8	83.87	123.01	83.39	0.013
L7-S11	36	2	R	E	25	30	0.52	117	0.12	2.5	2	19.4	44.2	58.68	58.51	64.76	0.008
L7-S12	36	1.5	R	E	25	32	0.68	116	0.12	2.5	2	19.4	45.2	57.35	77.35	63.66	0.011
L7-S13	36	1	R	E	25	36	0.98	111	0.11	2.5	2	19.4	47.2	54.99	111.02	61.58	0.016
L8-S10	36	2	R	E	25	47	0.50	113	0.12	2.5	2	19.4	52.7	50.01	56.51	56.59	0.009
L8-S11	36	1.5	R	E	25	43	0.67	114	0.12	2.5	2	19.4	50.7	51.62	76.01	58.29	0.012
L9-S4	36	1	R	E	25	75	0.94	106	0.11	3	2	21.0	69.0	42.35	106.02	46.01	0.020
L9-S6	36	0.5	R	E	25	38	2.09	118	0.12	3	2	21.0	50.5	53.95	236.04	58.44	0.036
L7-S2	51	1.5	RI	E	32	32	0.19	46	0.03	2.5	2	19.4	45.2	57.35	30.67	63.66	0.003
L7-S3	51	1	RI	E	32	36	0.37	60	0.04	2.5	2	19.4	47.2	54.99	60.01	61.58	0.006
L10-S2	36	0.8	R	L	25	33	1.33	113	0.12	2	4	11.7	34.0	56.72	150.69	79.13	0.017
L10-S3	36	0.5	R	L	25	22	0.12	7	0.01	2	4	11.7	28.5	65.53	14.00	90.58	0.001
L10-S7	36	1	C	L	22	44	1.09	123	0.04	2	4	11.7	39.5	51.20	123.02	70.54	0.015
L10-S8	36	0.8	C	L	22	33	0.06	5	0.00	2	4	11.7	34.0	56.72	6.67	79.13	0.001
L10-S9	36	0.5	C	L	22	22	0.14	8	0.00	2	4	11.7	28.5	65.53	16.00	90.58	0.002
L4-S10	36	2.5	C	L	22	11	0.42	119	0.04	2	2	17.5	31.8	83.87	47.61	83.39	0.005
L4-S14	36	1.5	C	L	22	9	0.43	73	0.02	2	2	17.5	30.8	90.08	48.67	85.46	0.005
L4-S2	36	2	I	L	32	9	0.50	112	0.02	2	2	17.5	30.8	90.08	56.01	85.46	0.006
L4-S3	36	1.5	I	L	32	9	0.66	112	0.02	2	2	17.5	30.8	90.08	74.67	85.46	0.008
L4-S6	36	2	R	L	25	9	0.69	157	0.16	2	2	17.5	30.8	90.08	78.51	85.46	0.008
L4-S8	36	1	R	L	25	11	0.58	65	0.07	2	2	17.5	31.8	83.87	65.01	83.39	0.007
L7-S10	36	1	C	L	25	36	1.01	114	0.03	2.5	2	19.4	47.2	54.99	114.02	61.58	0.016
L7-S14	36	2.5	R	L	25	26	0.39	111	0.11	2.5	2	19.4	42.2	61.75	44.41	67.10	0.006
L7-S15	36	2	R	L	25	30	0.54	123	0.13	2.5	2	19.4	44.2	58.68	61.51	64.76	0.008
L7-S17	36	1	R	L	25	36	1.11	126	0.13	2.5	2	19.4	47.2	54.99	126.02	61.58	0.018

Loading diagram code	$2r_b$ [mm]	*db* [m]	Rod type	Bond type	*rr* [mm]	*RQDw* [%]	τ*b* [MPa]	*Fb* [kN]	ε [%]	*Jr* [-]	*Ja* [-]	*JCond89* [-]	*GSI* [-]	Functions			
														q	*p*	*q´*	*p´*
L7-S8	36	2	C	L	22	30	0.47	106	0.03	2.5	2	19.4	44.2	58.68	53.01	64.76	0.007
L9-S10	36	1	C	L	22	75	1.42	161	0.05	3	2	21.0	69.0	42.35	161.03	46.01	0.031
L9-S11	36	0.8	C	L	22	56	1.88	159	0.05	3	2	21.0	59.5	46.99	212.04	51.54	0.036
L9-S12	36	0.5	C	L	22	38	1.04	59	0.02	3	2	21.0	50.5	53.95	118.02	58.44	0.018
L9-S3	36	0.5	R	L	25	38	2.02	114	0.12	3	2	21.0	50.5	53.95	228.04	58.44	0.035
L11-S11	51	0.5	RI	E	32	29	1.35	108	0.07	2.5	2	19.4	43.7	59.39	216.02	65.33	0.021
L11-S14	36	1	C	E	22	58	0.96	109	0.03	2.5	2	19.4	58.2	46.41	109.02	52.44	0.018
L11-S15	36	0.5	R	E	25	29	2.14	121	0.12	2.5	2	19.4	43.7	59.39	242.04	65.33	0.033
L11-S16	36	0.8	R	E	25	44	1.88	159	0.16	2.5	2	19.4	51.2	51.20	212.04	57.86	0.032
L11-S17	36	1	R	E	25	58	1.00	113	0.12	2.5	2	19.4	58.2	46.41	113.02	52.44	0.019
L11-S8	36	0.8	R	E	25	44	1.13	96	0.10	2.5	2	19.4	51.2	51.20	128.02	57.86	0.020
L11-S9	36	0.5	R	E	25	29	2.02	114	0.12	2.5	2	19.4	43.7	59.39	228.03	65.33	0.031
L12-S10	36	1	C	E	22	44	1.88	213	0.07	2	1	23.3	57.0	51.20	213.04	53.26	0.035
L12-S11	36	0.8	C	E	22	33	1.31	111	0.03	2	1	23.3	51.5	56.72	148.02	57.57	0.023
L12-S12	36	0.5	C	E	22	22	1.08	61	0.02	2	1	23.3	46.0	65.53	122.02	62.77	0.017
L12-S7	36	0.5	R	E	25	22	1.26	71	0.07	2	1	23.3	46.0	65.53	142.02	62.77	0.020
L12-S8	36	0.8	R	E	25	33	1.62	137	0.14	2	1	23.3	51.5	56.72	182.70	57.57	0.028
L3-S11	36	1	C	E	22	60	1.03	116	0.04	1.5	3	11.7	47.5	45.85	116.02	61.25	0.017
L3-S12	36	1	C	E	22	60	1.53	173	0.05	1.5	3	11.7	47.5	45.85	173.03	61.25	0.025
L3-S15	51	1	I	E	32	60	0.69	111	0.02	1.5	3	11.7	47.5	45.85	111.02	61.25	0.011
L3-S7	36	2	R	E	25	71	0.39	89	0.09	1.5	3	11.7	53.0	43.18	44.51	56.32	0.007
L3-S8	36	1.5	R	E	25	67	1.04	177	0.18	1.5	3	11.7	51.0	44.08	118.02	58.00	0.018
L3-S9	36	1.5	C	E	22	67	0.67	114	0.04	1.5	3	11.7	51.0	44.08	76.02	58.00	0.012
L5-S2	36	1	C	E	22	56	1.10	124	0.04	2	2	20.0	58.0	46.99	124.02	52.56	0.021
L5-S3	36	1.5	C	E	22	62	0.73	123	0.04	2	2	20.0	61.0	45.32	82.02	50.57	0.014
L6-S11	36	1	R	E	25	88	1.43	162	0.17	2	3	15.6	67.3	40.01	162.04	46.88	0.031
L6-S14	51	1.5	I	E	32	81	0.63	151	0.02	2	3	15.6	63.8	41.20	100.68	48.84	0.013
L6-S9	36	1.5	R	E	25	81	0.35	59	0.06	2	3	15.6	63.8	41.20	39.34	48.84	0.007
L12-S13	36	0.5	C	L	22	22	0.12	7	0.00	2	1	23.3	46.0	65.53	14.00	62.77	0.002
L12-S14	36	0.8	C	L	22	33	0.59	50	0.02	2	1	23.3	51.5	56.72	66.68	57.57	0.010
L12-S15	36	1	C	L	22	44	0.64	72	0.02	2	1	23.3	57.0	51.20	72.01	53.26	0.012
L12-S16	36	1	R	L	25	44	1.00	113	0.12	2	1	23.3	57.0	51.20	113.02	53.26	0.019
L12-S17	36	0.8	R	L	25	33	1.18	100	0.10	2	1	23.3	51.5	56.72	133.35	57.57	0.020
L12-S18	36	0.5	R	L	25	22	0.46	26	0.03	2	1	23.3	46.0	65.53	52.01	62.77	0.007
L3-S19	36	1	C	G	22	60	0.44	50	0.02	1.5	3	11.7	47.5	45.85	50.01	61.25	0.007
L3-S2	36	2	C	L	22	71	0.53	119	0.04	1.5	3	11.7	53.0	43.18	59.51	56.32	0.009
L3-S20	36	1	R	G	25	60	0.60	68	0.07	1.5	3	11.7	47.5	45.85	68.01	61.25	0.010
L3-S21	36	1	C	G	22	60	1.07	121	0.04	1.5	3	11.7	47.5	45.85	121.02	61.25	0.017
L3-S22	36	1	R	G	25	60	1.03	116	0.12	1.5	3	11.7	47.5	45.85	116.02	61.25	0.017
L3-S4	36	1.5	C	L	22	67	1.11	189	0.06	1.5	3	11.7	51.0	44.08	126.03	58.00	0.019
L3-S5	36	1	R	L	25	60	0.69	78	0.08	1.5	3	11.7	47.5	45.85	78.02	61.25	0.011
L3-S6	36	1	C	L	22	60	1.04	118	0.04	1.5	3	11.7	47.5	45.85	118.02	61.25	0.017
L5-S1	36	2	R	L	25	66	0.51	116	0.12	2	2	20.0	63.0	44.32	58.01	49.33	0.010
L5-S10	36	2	C	L	22	66	0.50	112	0.04	2	2	20.0	63.0	44.32	56.01	49.33	0.010
L6-S3	36	1.5	R	L	25	81	0.72	122	0.12	2	3	15.6	63.8	41.20	81.35	48.84	0.015
L6-S6	36	1	C	L	22	88	1.65	186	0.06	2	3	15.6	67.3	40.01	186.04	46.88	0.035
L1-S1	51	2.5	I	E	32	42	0.54	216	0.03	3	2	21.0	52.5	52.06	86.41	56.73	0.010
L1-S11	36	1	C	E	22	22	1.26	142	0.04	3	2	21.0	42.5	65.53	142.02	66.69	0.019
L1-S3	51	1.5	I	E	32	36	0.25	61	0.01	3	2	21.0	49.5	54.99	40.67	59.34	0.004
L1-S4	51	1	I	E	32	22	0.92	147	0.02	3	2	21.0	42.5	65.53	147.01	66.69	0.014
L1-S8	36	2	C	E	22	43	0.97	219	0.07	3	2	21.0	53.0	51.62	109.52	56.32	0.017
L2-S11	36	1.5	R	E	25	29	0.40	68	0.02	2.5	1	26.9	54.9	59.39	45.34	54.83	0.007
L2-S7	36	1	C	E	22	34	1.89	214	0.07	2.5	1	26.9	57.4	56.12	214.03	52.99	0.036
L1-S15	36	1.5	R	L	25	36	0.95	161	0.04	3	2	21.0	49.5	118.35	107.34	52.42	0.018
L2-S1	36	1	C	L	22	34	0.61	69	0.02	2.5	1	26.9	57.4	138.97	69.00	49.80	0.012
L2-S14	51	1	I	L	32	34	0.51	81	0.01	2.5	1	26.9	57.4	138.97	81.00	49.80	0.010
L2-S16	51	2	I	L	32	27	0.23	73	0.01	2.5	1	26.9	53.9	265.54	36.50	50.90	0.004
L2-S2	36	1.5	C	L	22	29	0.57	96	0.03	2.5	1	26.9	54.9	217.25	64.00	50.57	0.011

Note: rb: borehole diameter [mm], rr: rod diameter [mm], RQDw: weighted RQD1…n per db, Jr: joint rougness number, Ja: joint alteration number, JCond89: joint Condition rating, q and q´: regression functions, p and p´: objective functions, ε: strain of rod

In the third step the linearization of data was performed using objective functions p and p' in equations

$$p = \tau_b/q + F_b/d_b \tag{5}$$

and

$$p' = \tau_b/q' \tag{6}$$

where parameters q, q' were described by Eq. (2) and (3).

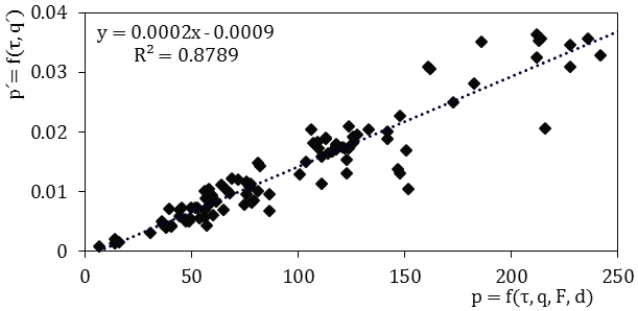

Fig. 4 Linearization of problem by objective functions p and p'

These functions were calculated (Tab. 3), plotted and fitted by linear curve (see Fig. 4) in the shape:

$$10^4\,\mathrm{p}' = 2\mathrm{p} - 9 \tag{7}$$

Now it was possible to substitute p´ from Eq. (6) and q´ from Eq. (3) which leads to:

$$\tau_b = \frac{2947(2\mathrm{p}-9)}{25000\ GSI^{0.77}} \tag{8}$$

and to substitute p from Eq. (5)

$$\tau_b = \frac{2947q(9d_b-2F_b)}{2d_b\left(2947-12500qGSI^{77/100}\right)} \tag{9}$$

and q from Eq. (2)

$$\tau_b = \frac{580559(9d_b-2F_b)}{2d_b\left(2947RQD^{9/25}-2462500GSI^{77/100}\right)} \tag{10}$$

which leads to initial solution in general form:

$$\tau_b = \frac{k_1(4.5d_b-F_b)}{d_b\left(k_2RQD_w{}^{k_3}-k_4GSI^{k_5}\right)} \tag{11}$$

where $k_{1\ldots5}$ [-] represents input iterative factors for sensitivity analysis. The value of *GSI* is given in Eq. (4) or by direct insertion.

3 SENSITIVITY ANALYSIS OF BOND FRICTION AND BOND MATERIAL

After the initial solution was assembled, a sensitivity analysis was required. For this purpose, the conjugate gradient (CG) method with line search was used. As the determining function, it was chosen to perform the sum of squared differences (SSD) of approximate and experimental bond friction as:

$$\mathrm{SSD} = \min_{\tau>0} \sum_{i=1}^{n} \left(\tau_{approx_i} - \tau_{exp_i}\right)^2 \tag{12}$$

with the convergent criterion $\|\mathrm{SSD}^{(k+1)} - \mathrm{SSD}^{(k)}\| < 10^{-4}$. In order to distinguish the influence of bond material, this data had to be solved separately. The initial condition factors were taken from Eq. (10). The achieved initial results can be seen in the left half of Tab. 4.

Table 4. Results of sensitivity analysis of bond friction and bond materials

	Input →		→ Initial results		Input →	→ Final results		
Factor	**Initial solution	Bond type E by sealing	Bond type E by grouting	Bond type L by mixing	***Final solution	Bond type E by sealing	Bond type E by grouting	Bond type L by mixing
k_1	580559	76405.56	49351.14	81248.68	*1000UCS_{mean}	57000 const.	51000 const.	44000 const.
k_2	2947	2953.59	2944.36	2936.59	*ρ_{mean}	2539 const.	2550 const.	2474 const.
k_3	9/25	0.363	0.360	0.358	1/2		const.	
k_4	2462500	8390779.58	7635379.64	8138386.27	initial k_4	1695651.30#	2289071.07#	1292695.52#
k_5	77/100	0	0	0.022	1/3		const.	
SSD	17.71	0.012	0.002	0.015	-	0.105	0.036	0.117

Note: SSD: sum of squared differences,
*) mean value for relevant solved data set, **) from Eq. (10), ***) to Eq. (13), #) to Eq. (15)

The results show that factor k_5 is reduced to zero, which would mean missing the *GSI* value. In addition, during the linearization (Eq. 7), ρ_{vmean} and UCS_{mean} were lost, which was not originally intended. From the initial results of the factors k_1 and k_2, it was obvious that they could be approximated after the resetting. In the next step, therefore, the ρ_{vmean} and UCS_{mean} were used as constant values. The factor k_5 was replaced by 1/3 in order not to lose the GSI value for next analysis. The factor k_3 was replased for simplicity 1/2. As a variable, therefore, the only factor k_4, representing the influence of bond material, was solved in the final solution. The achieved final results can be found in the right half of Tab. 4. The insertion of factors $k_{1...5}$ from the final solution into the equation (11) yields:

$$\tau_b = UCS_{mean} \frac{4.5d_b - F_b}{d_b(\rho_{mean}\sqrt{RQD_w} - k_4 \sqrt[3]{GSI})} \tag{13}$$

with UCS_{mean} for simplicity in kPa. For other applications, factor k_4 was rounded to adequate accuracy 10^5, achieved SSD have not changed.

The summary of results is represented by scatter diagrams. The initial state shows Fig. 5a, where the imbalance between the measured and calculated bond friction values is seen. This is the entire set of data for n = 87. The final results (Fig. 5b,c,d) were obtained after solving one variable k_4. The accuracy of bond friction values ranged between 0.01 and 0.02 MPa of the mean absolute difference values.

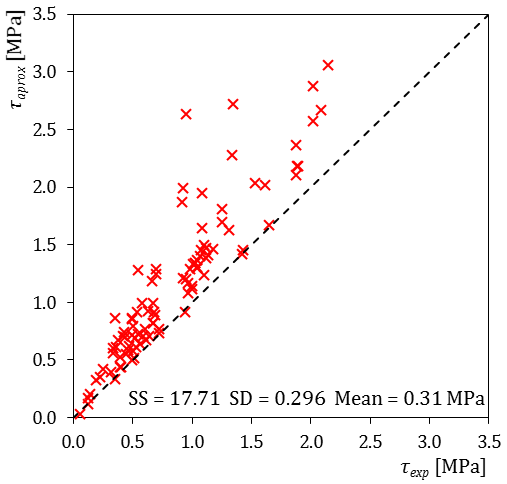

a)

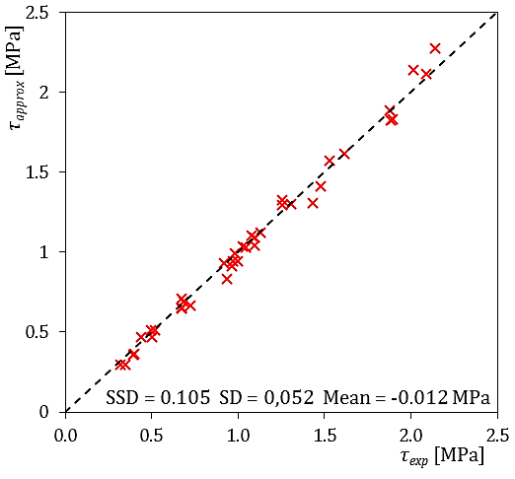

b)

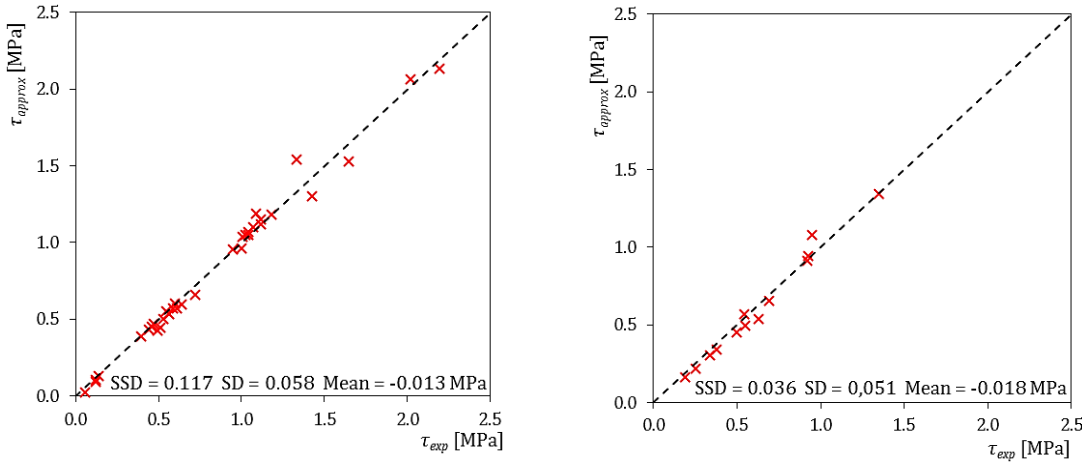

c) d)

Fig. 5a,b,c,d Scatter diagrams of calculated and experimental bond friction for init. solution: (a) all data set and for final solution: (b) cem. sealing, (c) cem. grouting, (d) resin cartridge mixing.

4 SENSITIVITY ANALYSIS OF BOND LENGHT

A sensitivity analysis of bond length was made on the basis of conclusions published by Hobst and Zajíc [9]. During the loading tests, the authors found little changes in the bond area (cement sealing in intact rocks) in relation to large changes in bond friction. While a bond area increased, the bond friction changes were already insignificant. The experimental data here show similar behavior, as shown below.

As stated earlier, the results of load tests and their interpretation are the product of many variables. For example, we can project bond friction against bond length (Fig. 6a) and generally we can see the above-mentioned non-linear behaviour. Since the bolt holes were drilled in three different diameters (see Table 3), it is correct to project the bond friction against the bond area, the trend is very similar (Figure 6b).

a)

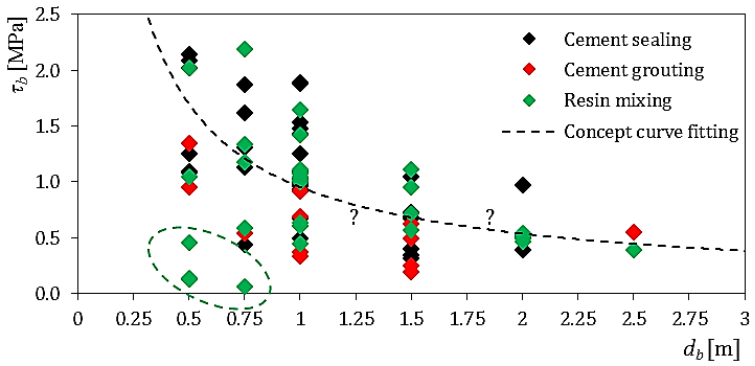

b)

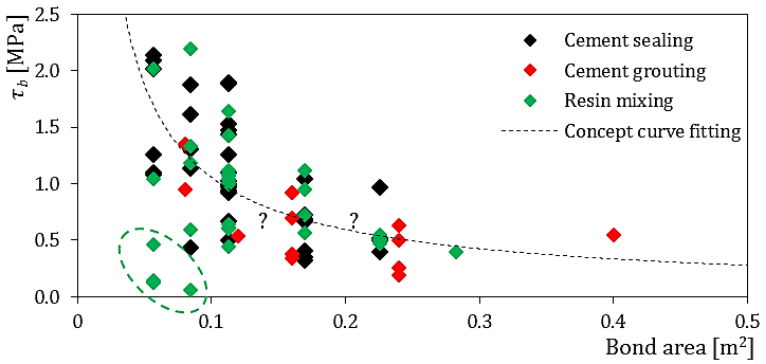

Fig. 6a,b Bond friction in relation to bond length (a); bond friction in relation to bond area (b); green ellipse borders poor mixing of resin cartridge

It can be seen that scattering of the bond stress can be caused by selected parameters such as the strength and jointing of rock mass, bonding material and the size of the bond failure force. The basic idea of the

sensitivity analysis of the bond length was to search for the interaction and certain robustness between the selected parameters. For this purpose, the Monte Carlo (MC) method in Hillar and Pruška [10] with the uniform and normal distribution of variables were used.

Initially, it was necessary to obtain input values using simple statistics (Tab. 5). For the uniform distribution, it was necessary to set upper and lower limits of the variables, for the normal distribution it was necessary to set the mean and standard deviation.

Table 5. Input values for generation of pseudo-random numbers

	Cement sealing					Cement grouting					Resin mixing				
	UCS_{mean}	ρ_{mean}	RQD_W	GSI	τ_b	UCS_{mean}	ρ_{mean}	RQD_W	GSI	τ_b	UCS_{mean}	ρ_{mean}	RQD_W	GSI	τ_b
Mean*	56.61	2538.50	45.84	51.03	1.08	51.38	2550	41.85	45.51	0.63	43.74	2474.12	45.74	50.10	0.83
SD*	20.033	226.263	17.067	7.559	0.525	28.858	236.157	21.965	8.694	0.330	20.741	226.691	18.699	10.632	0.507
Min**	29	2016	22	34	0.32	6	2016	21	28.5	0.19	6	2016	22	28.5	0.06
Max**	86	2869	88	69	2.14	86	2869	83	63.8	1.35	74	2690	88	70.5	2.19

Note: SD: standard deviation, *) normal distribution, **) uniform distribution

This data formed the basis for generating pseudo-random numbers. A linear congruential generator (LCG) was used for this purpose in relation $u_{i+1} = (au_i + c) \bmod m$ for random seed $0 \leq u_0 < m$, where multiplier $a = 1140671485$, increment $c = 12820163$ and modulus $m = 2^{24}$. Sampling was used for standard uniform distribution where $\boldsymbol{f}(x) = x_{min} + (x_{max} - x_{min})u$ for $0 \leq u \leq 1$. The normal distribution is a continuous probability distribution. It is defined by the probability density function (PDF):

$$f(x) = \frac{1}{\sigma\sqrt{2\pi}} \mathrm{e}^{-\frac{(x-\mu)^2}{2\sigma^2}} \tag{14}$$

where the parameter μ is the mean and the parameter σ is the standard deviation. The variable x is defined by using LCG for the probability of 95.45 %. In the first step we obtain standard uniform random values U (0;1) from the generator and in the second step is needed to transform the data by probit function $probit(p) = 2^{1/2}\,\mathrm{erf}^{-1}(2p - 1)$ where erf is Gauss error function. Being sufficiently representative the random process was chosen $n = 1500$ samples.

After generating the random variables (see input values from Tab. 5), a bond length simulation was performed, which was expressed from Eq. (11) to form:

$$d_b = \frac{F_b UCS_{mean}}{4.5UCS_{mean} - \tau_b(\rho_{mean}\sqrt{RQD_W} - k_4\sqrt[3]{GSI})} \tag{15}$$

with UCS_{mean} for simplicity in kPa, parameter $k_4 = 17.10^5$ for cement sealing; 23.10^5 for cement grouting and 13.10^5 for resin mixing (rounded by Tab. 4 on the right), F_b = const. value (25; 50; 75; 100; 150; 200; 250) kN. The values of the bond length were plotted against the bond friction at const. F_b for a total of three used bond materials. The output of one of the three cases can be seen in Fig. 7a,b. As can be seen, the normal distribution data more closely corresponds to all possible conditions that may occur in situ. By contrast, the uniform distribution data is much more conservative with regard to the fixed boundaries and constant probability density.

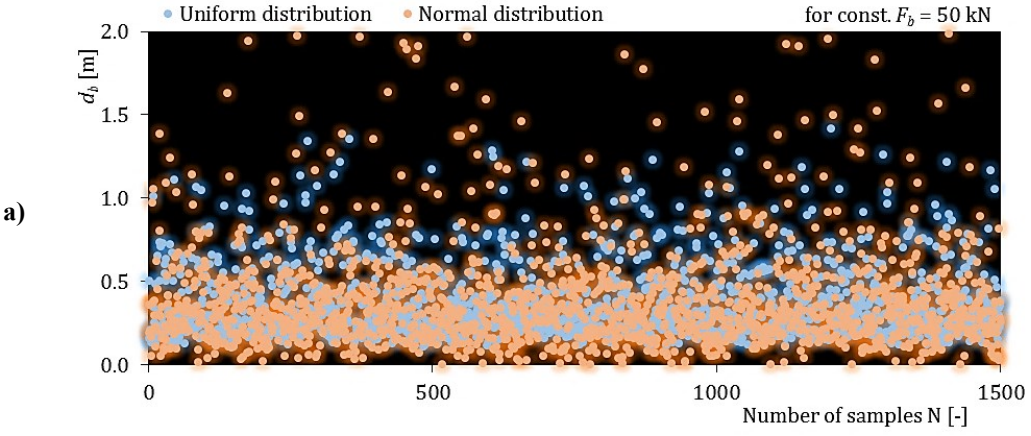

a)

b)

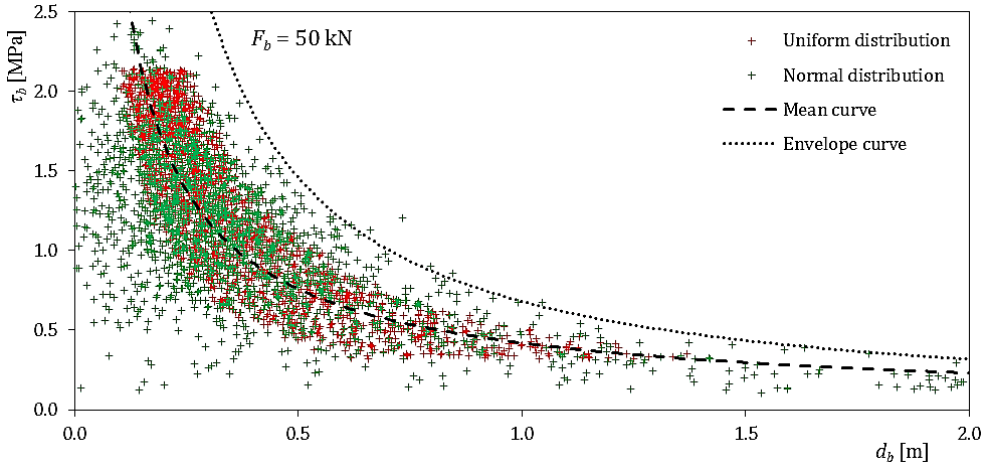
F_b = 50 kN
Uniform distribution
Normal distribution
Mean curve
Envelope curve
τ_b [MPa]
d_b [m]

c)

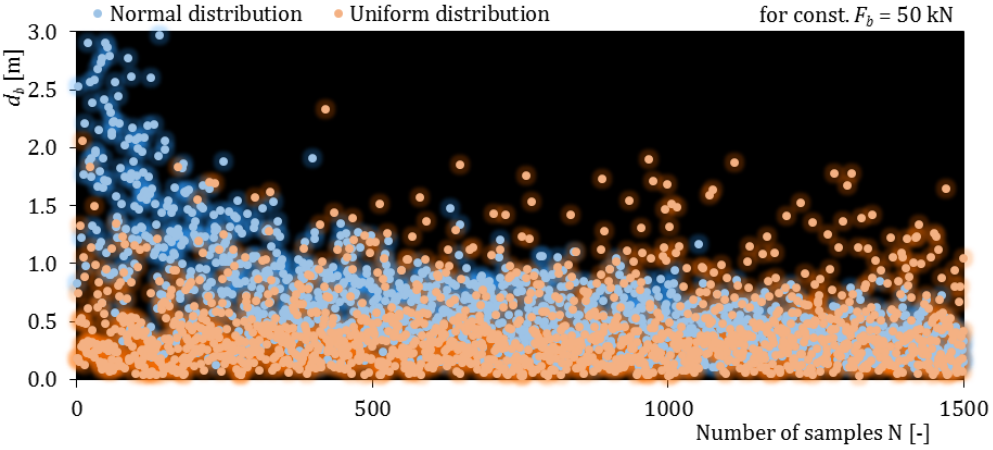
Normal distribution
Uniform distribution
for const. F_b = 50 kN
d_b [m]
Number of samples N [-]

d)

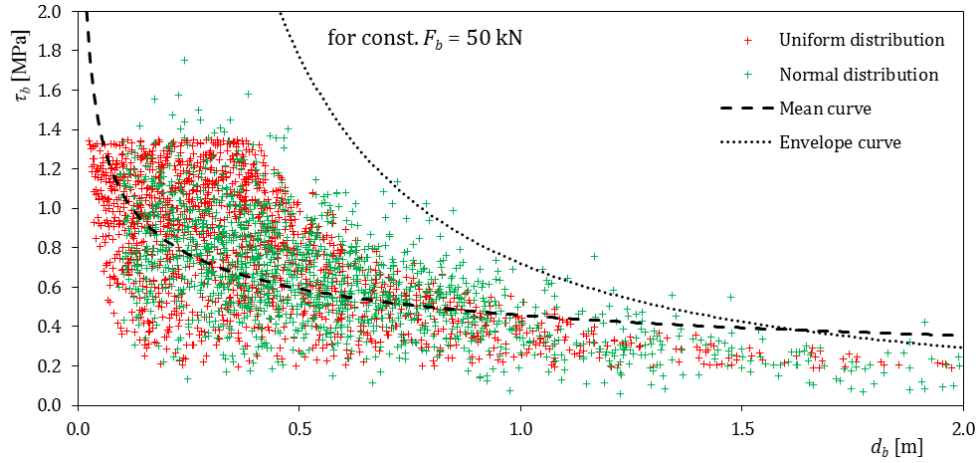
for const. F_b = 50 kN
Uniform distribution
Normal distribution
Mean curve
Envelope curve
τ_b [MPa]
d_b [m]

e)

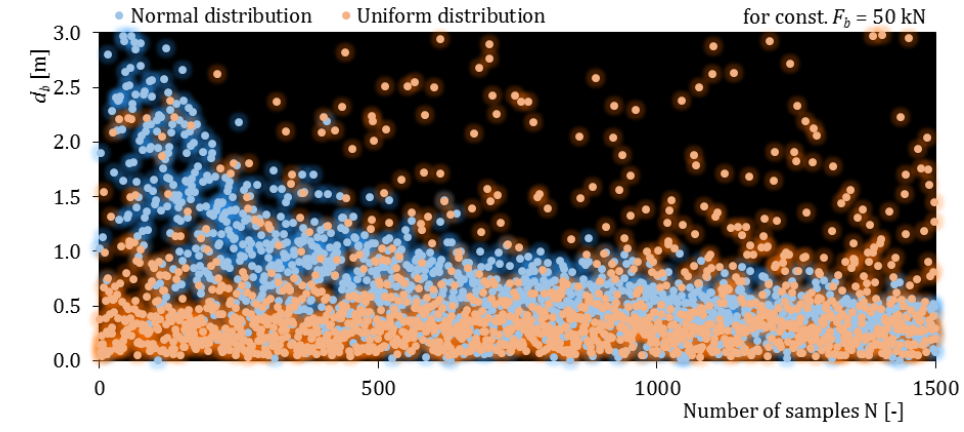
Normal distribution
Uniform distribution
for const. F_b = 50 kN
d_b [m]
Number of samples N [-]

f)

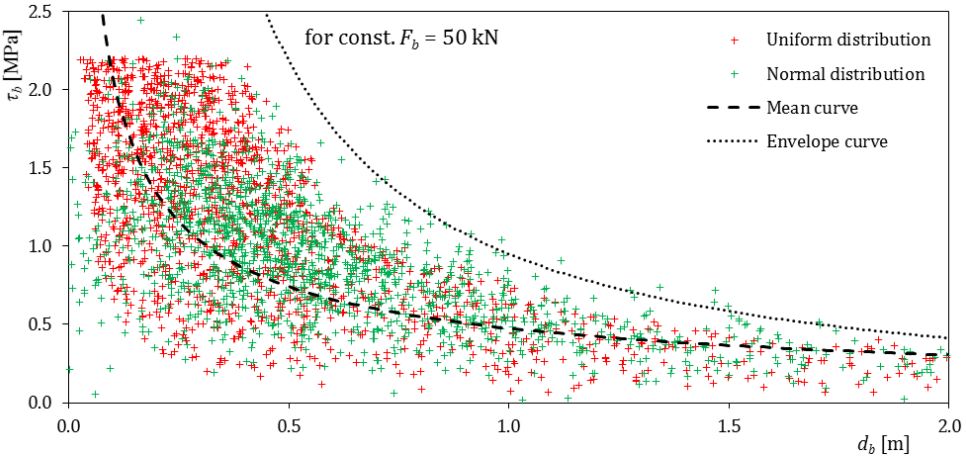

Fig. 7a,b,b,c,d,e Example of bond length in relation to number of samples (a, c, e); bond friction in relation to bond length (b, d, f); simulation here by constant F_b = 50 kN and cement sealing type of bond (a, b); cement grouting (c, d); resin cartridge mixing (e, f)

The sensitivity analysis was interpreted by the numerical approximation of the uniform data by the best fit power function and normal data by the envelope power function in the modified form $d_b = a\tau_b^b$ (14), where a,b [-] are constants. It should be noted that all the tests were carried out with two bore diameters (see Table 3). For full treated rods and fiberglass rods (cement sealing and resin mixing) was used diameter 36 mm and diameter 51 mm for self-drilling rods (cement grouting). The calculated bond length thus corresponds to one of these cases. If we consider a different drilling diameter, it is necessary to convert it over an equivalent surface A' (part 2).

5 RESULTS AND USE

By summarizing the sensitivity analysis of the bond friction and the bond length (part 3 and 4) and interpreting the data, the following results were reached. There are two ways to use the results. First of all, it is possible to say that we have a geotechnical survey and, secondly, that we only have a rough estimate of the data. In the first (and better) case, when the geotechnical data is available, it is possible to determine e.g. the bond length directly from Eq. (15). By inserting a typical bond friction from Tab. 2 or other database we get the bond length value for a bond failure force. The magnitude of this force (according to the safety factor) must be in the interval (F_{ed}, F_{yd}) where F_{ed} is the design anchor force and F_{yd} is the yield strength of the steel rod or the strength of the composite thread.

Let's take these parameters available from the case study: an unstable rock block with a single rock bolt, loading F_b from the static report $1.5F_{ed}$ = 136 kN, the rock bolt will be bonded by cement sealing in jointed granite, estimated bond friction 0.75 MPa, drill core 3.0 m with the mean UCS = 74200 kPa, ρ_v = 2651 kg.m^{-3}, RQD_{300} = (45+51+86), for expected bond length to 1.0 m is $RQDw = 45d_b$; to 2.0 m is $(45+51(d_b-1))/d_b$; to 3.0 m is $(45+51+86(d_b-2))/d_b$ and so on, the mean ratio J_r/J_a = 2/4 and given RQD_w tends to GSI by Eq. (4). The imbalance between the calculated bond length and the previous RQD_w and GSI will be solved by a fixed-point iteration or by a trial and error method. The result here is d_b = 2.13 m.

It is now necessary to anchor the block with the same loading F_b = 136 kN hypothetically, for example, on the opposite side of the railway cutting with a better quality of granite with the same estimate of bond friction 0.75 MPa with mean UCS = 78100 kPa, ρ_v = 2695 kg.m^{-3}, RQD_{300} = (65+79+76) and J_r/J_a = 3/1. The result here is d_b = 1.86 m. The difference in results is 0.27 m, so 12.7% saving of materials, drilling, time and money due to consideration of geological conditions (still the same bond friction). In fact, the bond friction should be increased in less weathered granite. For example, when increasing to 1.0 MPa, the bond length is already reduced by 0.71 m. Especially for a steel mesh installation, this optimization of anchor elements is significant.

Another situation occurs if a detailed geotechnical survey is not carried out. Then it is possible to use the interpretation of the results of the bond length sensitivity analysis (part 4) represented by correlation coefficients (Tab. 6).

Table 6. Correlation coefficients for estimating of bond length

	Uniform distribution									Normal distribution					
	Cement sealing			Cement grouting			Resin mixing			Cement sealing		Cement grouting		Resin mixing	
F_b	a	b	R^2	a	b	R^2	a	b	R^2	a	b	a	b	a	b
25	0.24	-0.84	0.81	0.25	-0.57	0.49	0.32	-0.66	0.59	0.35	-1.01	0.32	-1.42	0.42	-1.22
50	0.43	-0.84	0.82	0.37	-0.58	0.49	0.48	-0.65	0.59	0.68	-1.10	0.72	-1.31	0.95	-1.20
75	0.61	-0.84	0.81	0.47	-0.58	0.49	0.63	-0.63	0.62	1.05	-1.05	1.11	-1.33	1.40	-1.05
100	0.77	-0.83	0.82	0.55	-0.59	0.49	0.75	-0.64	0.57	1.39	-1.03	1.41	-0.95	1.95	-1.05
150	1.07	-0.84	0.80	0.71	-0.59	0.49	0.96	-0.62	0.58	1.95	-0.83	1.92	-0.85	2.60	-0.92
200	1.37	-0.84	0.81	0.83	-0.57	0.49	1.17	-0.64	0.60	2.41	-0.85	2.33	-0.81	3.05	-0.81
250	1.65	-0.85	0.82	0.95	-0.58	0.49	1.38	-0.65	0.59	2.82	-0.75	2.72	-0.80	3.35	-0.65

Note: a,b: constants, R^2: coefficient of determination

The resulting correlations have been converted into design diagrams where the type of bond material and the resulting data distribution are available. Less realistic estimates provide diagrams with the uniform distribution that are slightly higher than the mean of the normal distribution for 1σ. On the other hand, the envelope curves in diagrams with normal distribution provide safe conservative values with more than 95.45% probability. For example, we are looking for a bond length of a rock bolt from the previous case study. We deduct $d_b \approx 1.3$ m (too optimistic, risk) from Fig. 8a, and $d_b \approx 2.5$ m (too conservative, total save) from Fig. 8b. The truth lies somewhere in between, and this is just another argument for carrying out a detailed geotechnical survey.

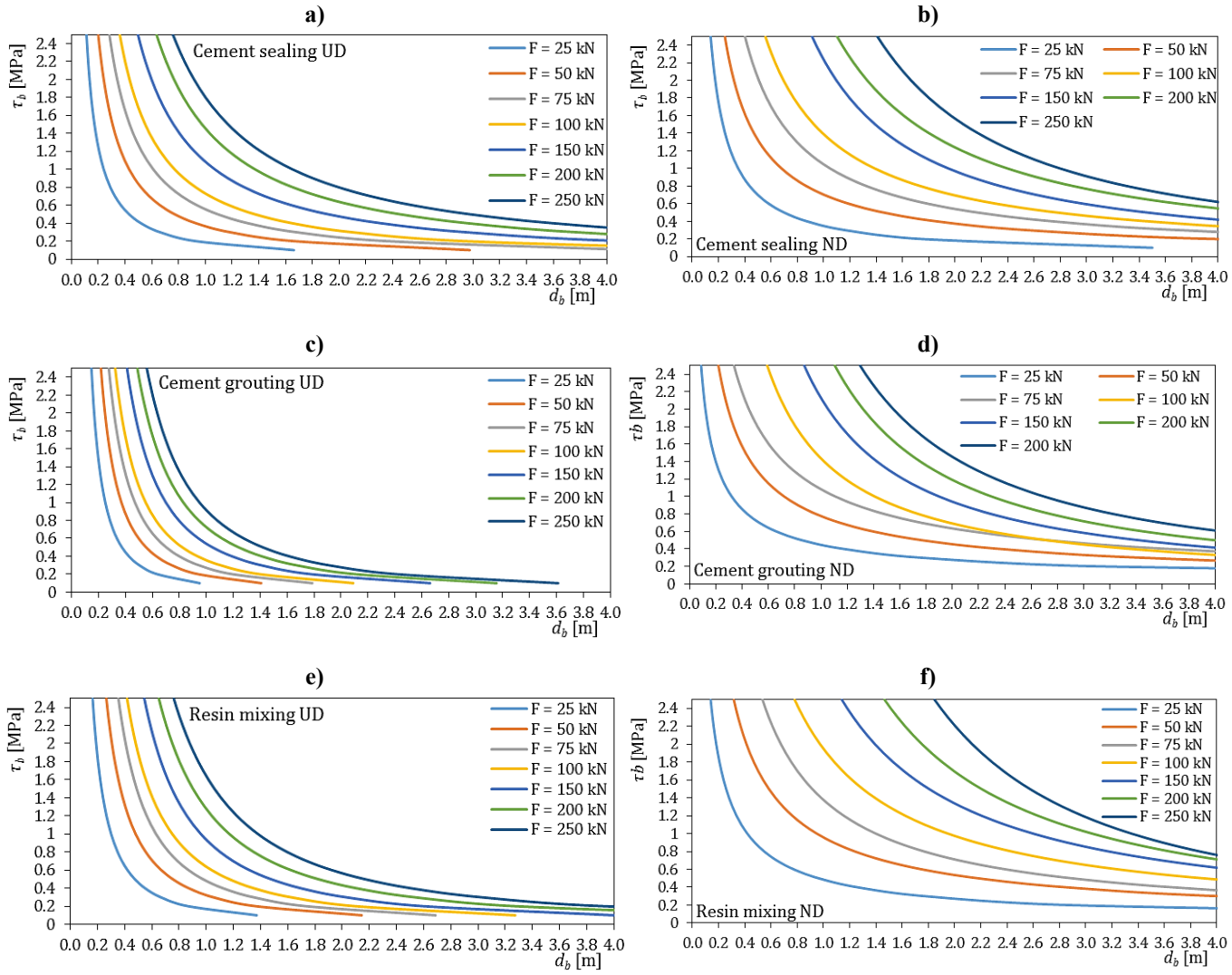

Fig. 8a,b,c,d,e,f Design diagrams of bond length in relation to bond friction (UD: uniform distribution, ND: normal distribution); (a,b) cement sealing (c,d); cement grouting; (e,f) resin mixing cartridge

6 CONCLUSIONS

In the paper, the in situ loading tests were mentioned. A summary of the tested localities and the results of the laboratory testing are given in Tab. (1). The process of obtaining experimental data and sorting was described. Then the description of the chosen model of the bond friction sensitivity analysis followed. The sensitive analysis was performed by using conjugate gradient method with the mean deviation of maximum 0.02 MPa of the absolute difference values. The process of simulation of randomly generated variables was followed by observation of non-linear behaviour of the bond length and bond friction. The result is, on the one hand, the possibility of direct calculation of the bond length considering a change of geological condition or on the other hand the use of design diagrams. The results are demonstrated by a simple case study where both approaches are compared. The importance of the bolt length optimization is simply quantified.

ACKNOWLEDGEMENTS

The work was supported by Ministry of Industry and Trade with program grant code FR-TI4/329 Research and Development - creation of an application system for the design and assessment of earth and rock anchors, including the development of monitoring elements.

Conflicts of Interest: The author declares that he has no conflict of interest.

REFERENCES

[1] HOLÝ, O. Evaluation of many load tests of passive rock bolts in the Czech Republic. *Geoscience Engineering*. 2017. Vol 63, No 1. pp. 1 -7. ISSN 1802-5420.

[2] PALMSTRÖM, A. Measurements of and Correlations between Block Size and Rock Quality Designation (RQD). *Tunnels and Underground Space Technology*. 2005. Vol 20, p. 362-377.

[3] KIM, M.K. and P.V. LADE. Modelling rock strength in three dimensions. *International Journal of Rock Mechanics and Mining Sciences & Geomechanics Abstracts*. 1984. Vol.21, No.1, pp. 21-33.

[4] DEERE, D.U. *Rock quality designation (RQD) after 20 years*. U.S. Army Corps Engrs. Contract Report GL-89-1. Vicksburg, MS: Waterways Experimental Station. 1989.

[5] LITTLEJOHN, G. S. and D.A. BRUCE. *Rock Anchors—State of the Art*. Foundation Publications Ltd., Brentwood, Essex, UK. 1977.

[6] WYLLIE, D.C. and C.W. MAH. *Rock Slope Engineering*. 4th ed. New York. 2014, ISBN 0-203-57083-9.

[7] LI, C. and B. STILLBORG. Analytical model for rock bolts. *Inter. Jour. of Rock Mechanics and Mining Sciences*. 1999. Vol 36, p. 1013 - 1027.

[8] HOEK, E. et al. Quantification of the Geological Strength Index Chart. *47th US Rock Mechanics/Geomechanics Symposium*. San Francisco. ARMA. 2013.

[9] HOBST L. and J. ZAJÍC. *Anchoring in Rock and Soil.* 1983. 2nd Edition. ISBN: 9780444600776.

[10] HILLAR, M. and J. PRUŠKA. *Využití statistiky pro numerické modelování podzemních staveb (Using statistics in numerical modelling of underground structutres)*. Konf. geotechnické problémy líniových stavieb. Bratislava. 2011. 8 p.